PROCEEDINGS, 41st Workshop on Geothermal Reservoir Engineering
Stanford University, Stanford, California, February 22-24, 2016
SGP-TR-209

A Reservoir Simulation of the Muara Laboh Field, Indonesia

Jantiur Situmorang, Rudy Martikno, Alfianto Perdana Putra, Novi Ganefianto

Supreme Energy, Menara Sentraya 23rd Floor, Jakarta 12160

jantiur-situmorang@supreme-energy.com

Keywords: Muara Laboh, Reservoir Simulation, Dual Porosity, PetraSim

ABSTRACT

This paper describes the application of reservoir simulation to evaluate the fracture permeability distributions as well as to forecast future reservoir performance of the Muara Laboh Geothermal Field. Data from six full diameter exploration wells were used in the evaluation. Dual porosity approach was implemented using PetraSim. Reservoir model was coupled with wellbore model to complete forecast simulation.

1. INTRODUCTION

Muara Laboh Geothermal Field is located in South Solok Regency, West Sumatra, Indonesia. The prospect is situated along the segment of the Great Sumatra Fault. Three principle surface manifestations, including Patah Sembilan (PS) fumaroles to the south, Idung Mancung (IM) fumaroles in the middle, and Sapan Malulong (SM) springs to the north define the presence of geothermal potential in the area. The later geological, geochemical, and geophysical surveys, as well as gradient-hole drilling delineate the potential extension of the geothermal system. Figure 1 presents the location of the Muara Laboh field, and its surface features distribution. The blue line in Figure 1 indicates boundary between concession area to the north and the national forest to the south.

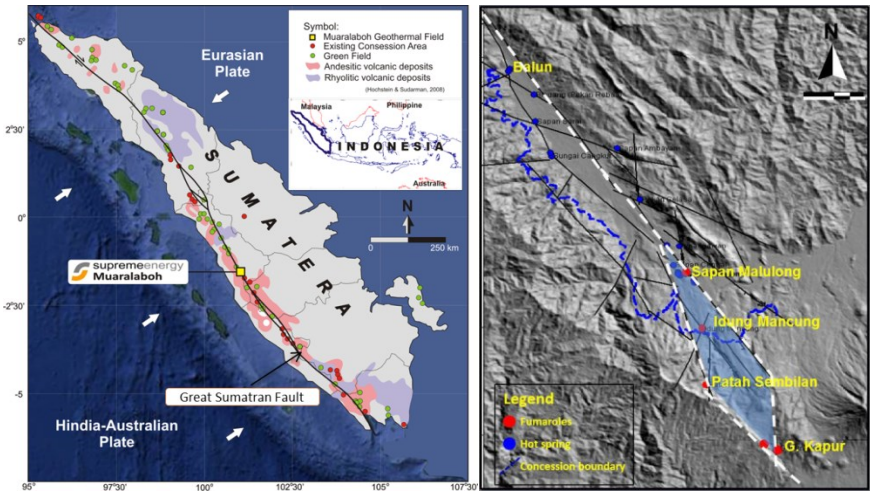

Figure 1: Location and surface features of Muara Laboh Geothermal Field

In 2012-2013 PT Supreme Energy Muara Laboh (SEML) drilled six full diameter exploration wells. All wells were drilled directionally from the well-pad located within the concession area. Two of them were completed within geothermal reservoir to the south, underneath the national forest. The results of the exploration have been used to define the temperature distributions, resource size, permeable structures, and hydrology of the system. At the initial state, it appears that hot geothermal fluid is upwelling from the deep part of the resource to the south, close to the PS fumaroles. The fluid flows to northwest along the path almost parallel to NW-SE structures. When fluid reaches just north of Pad-H, it turns to follow NE-SW permeable structures, passing ML-A1 well, to Idung Mancung (IM) fumaroles before it then flows toward Sapan Malulong (SM) springs to the north along the NNW-SSE permeable structures. Throughout its movement from the southern upwelling to the northern outflow, the reservoir fluid experiences a temperature decrease from 310^{o}C to 200^{o}C

In the most part, the reservoir contains a single phase liquid. A small developed steam cap exists in the shallow part of the reservoir, beneath IM fumaroles as confirmed by one of the exploration wells. The field conceptual model is illustrated in Figure 2.

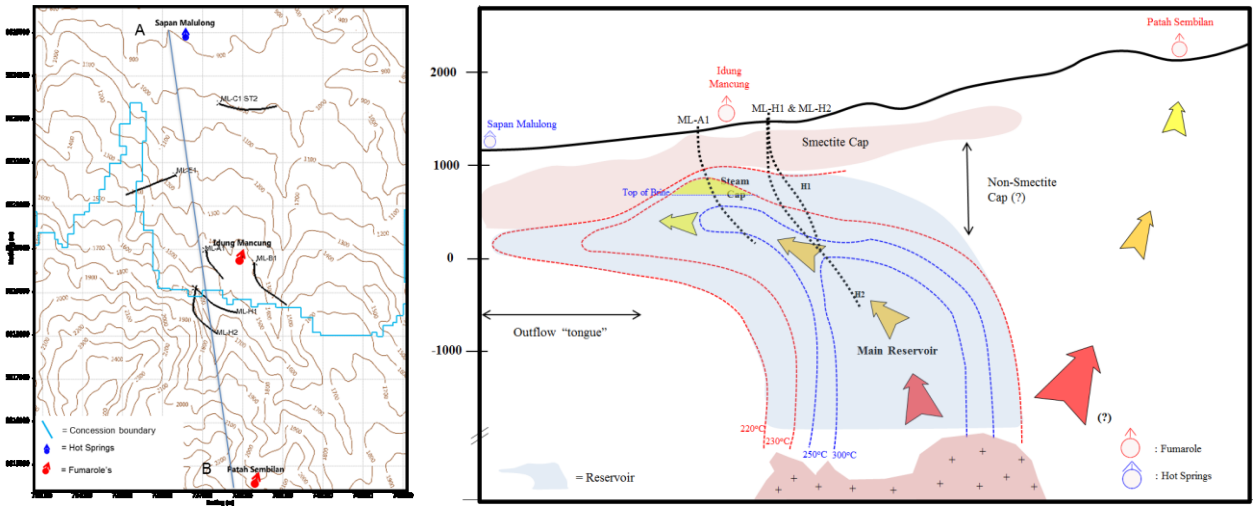

Figure 2: North-south cross section showing conceptual model of Muara Laboh field

During the course of exploration drilling program, the comprehensive well testing program including pressure-temperature (PT) surveys, pressure-temperature-spinner (PTS) surveys, and interference test were conducted, providing fundamental information needed for reservoir evaluation. The well testing information gathered has been used to verify the numerical model of the field previously constructed. Through model calibration processes, the fracture permeability distribution of the model was reassessed. Once the reservoir model has been well calibrated, it was then used to forecast reservoir response to exploitation.

Reservoir simulation is very time consuming and offers a non-unique solution with a high degree of uncertainty. With the intention to providing a careful recommendation for field development plan, the Muara Laboh Numerical Model was built deterministically by applying these following approaches:

1. All possible lateral or horizontal reservoir extensions delineated by Geophysics, Geology and Geochemistry information but have not been proven by drilling were treated as non-reservoir. Most of the potential extension comprises the part of resources beneath the national forest, far to the south, that presently cannot be accessed by drilling from the concession area.

2. Reservoir area, thickness, and permeability structures assigned in the model were constrained by the measured wells' pressure and temperature, and reservoir information collected during the interference test. The reservoir parameters for the model were obtained through a process involving a lot of iterations of model calibration.

3. Conservative values were assigned to the parameters that are poorly constrained such as matrix permeability, porosity, fracture spacing, and fracture porosity. The values assigned are based on the other similar geothermal fields.

PetraSim, a pre- and post-processor for TOUGH2, was used to develop the reservoir model using dual porosity approach. In addition to PetraSim, separate functions and modules were created in Microsoft Excel Visual Basic for Applications (VBA) to accomplish the reservoir simulation process. In the following paragraphs the workflow of Muara Laboh Reservoir Simulation is presented.

2. NUMERICAL MODEL DESCRIPTION

2.1 Model Grid

The grid of the model is aligned at N 12° W, covering a total area of 12 km x 17 km or equal to 204 km^2 and a total thickness of 3 km (i.e. from 1200 masl to –1800 masl). The grid block horizontal dimension varies from the smallest 200 m x 200 m to the biggest 1000 m x 1000 m. The model is divided into 13 layers; each layer is 200 m thick, except for layer 12 & 13 which are 400 m thick. Total number of blocks is 22542. As it is a dual porosity model , each block has porosity and permeability elements both in the matrix and in the fractures, and thus yielding a total active elements of 45084. A 3D visualization of the model grid blocks is presented in Figure 3.

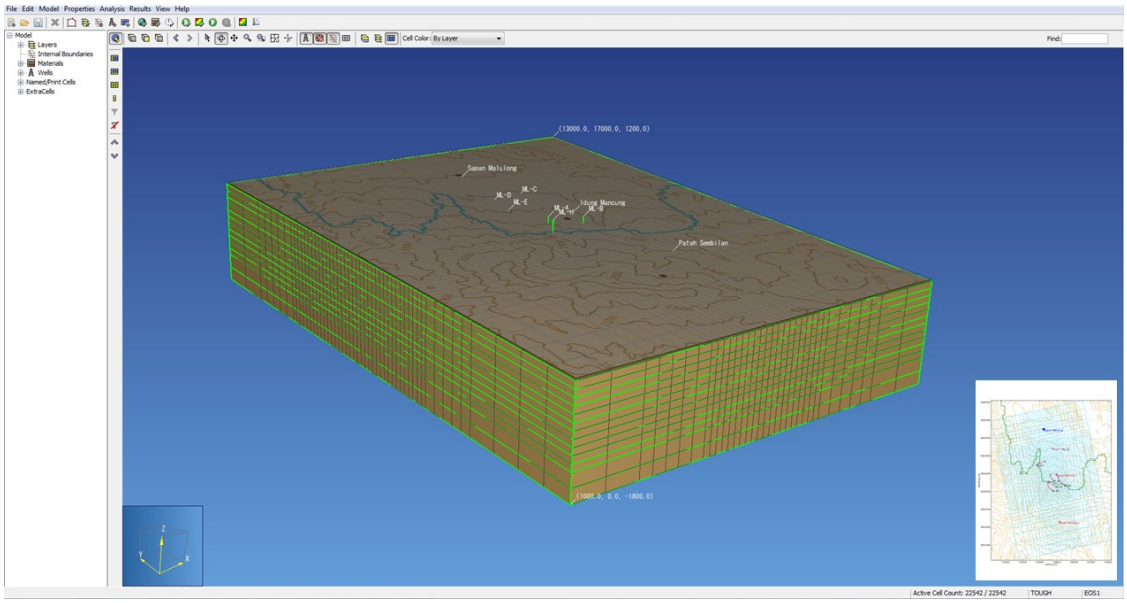

Figure 3: 3D view of Muara Laboh numerical model

2.2 Boundary Conditions

The top layer is put in a contact with an impermeable atmospheric block at surface elevation to allow conductive heat loss out of the reservoir. In PetraSim, this configuration is activated by adding an extra cell, to which the upper most blocks are connected (Figure4). The pressure and temperature of the extra cell are 1.013E5 Pa and 20^{o}C respectively, referring to atmospheric conditions. To prepare the detail input parameters for connection (i.e. orientation, distance, area, gravity, etc.), a separated function in Excel spreadsheet was created. IM and SM natural discharges are modeled by putting in artificial wells on deliverability at a constant wellbore pressure. Hot water with constant enthalpy and mass rate is injected into the southern base reservoir (Figure 5) to represent a deep heat flux to the system. The amount of the deep up-flow recharge obtained from initial state calibration was 36 kg/s at an enthalpy of 1500 kJ/kg. The lateral boundaries are assigned to be impermeable.

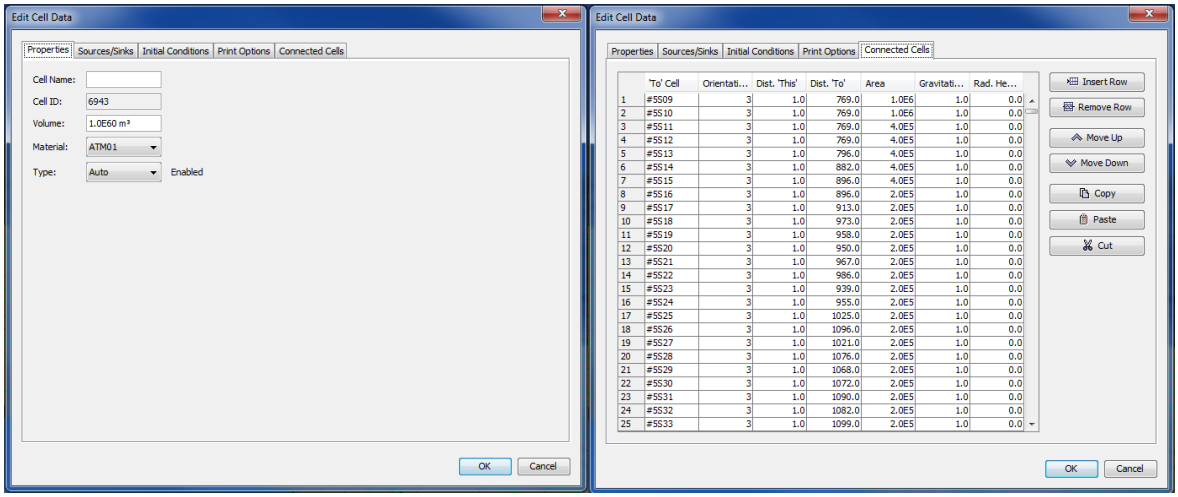

Figure 4: Top boundary condition implementation in PetraSim by using extra cell

2.3 Rock Properties

Matrix porosity, matrix permeability, fracture spacing, and fracture volume fraction assigned in the model are 5%, 0.02 mD, 100 m, and 1% respectively. Grant's curves of relative permeability and linear capillary pressure functions are applied in the calculation. To all rock types, the density, wet heat conductivity, and specific heat are specified to 2600 kg/m^3, 2 W/(m^{o}K), and 1000 J/(kg^{o}K).

Rock materials in the model are specified mainly upon different fracture permeability. In general, the rock distribution is illustrated in Figure 5 and described in Table 1. These fracture permeability distribution were obtained from over a hundred times of trial and error

until natural state and production history matching are achieved. The permeability values obtained through this iteration process is comparable to the values reported in some other volcanic hosted geothermal fields such as Ogiri Geothermal Field (Itoi et al., 2010) , and on the other fields that the authors have worked before.

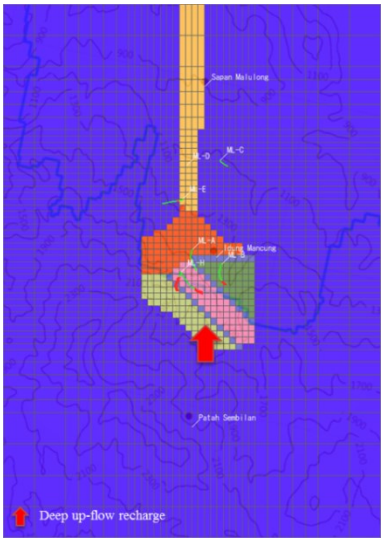

Rock	Color	Kx, ky, kz (mD)	Top, bottom (masl)
ROCK1		0.02, 0.02, 0.02	1100, -1600
ROCK2		0.01, 200, 200	700, -500
ROCK3		280, 340, 500	700, 100
ROCK4		5, 5, 20	-100, -1600
ROCK5		35, 35, 100	300, -1600
ROCK6		10, 10, 20	100, -1600
ROCK7		0.002, 0.002, 0.002	100, -1600

Figure 5: Simplified rock distribution

3. NUMERICAL MODEL CALIBRATION

3.1 Initial State Calibration

During the initial state calibration, also called natural state modeling, the computer model was run for 100.000 years until pseudo steady state conditions were reached. The results were then compared against actual wells temperatures and pressures. To obtain a good fit between model results and field data, the fracture permeability structures, and the rate and enthalpy of deep recharge were adjusted in an iterative process.

The results of the natural state calibration are summarized in Figure 6. Pressure and temperature in the model have been successfully matched against the measurements. Figure 7 presents a north-south cross section of the model natural state temperature, showing a good agreement with the conceptual model previously presented in Figure 2.

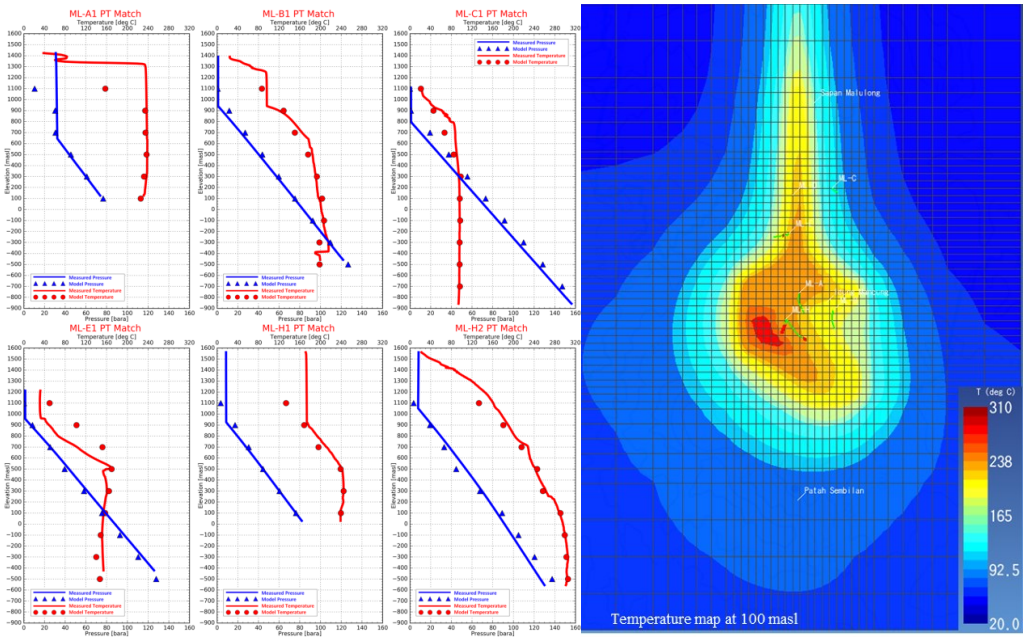

Figure 6: Natural state calibration results.

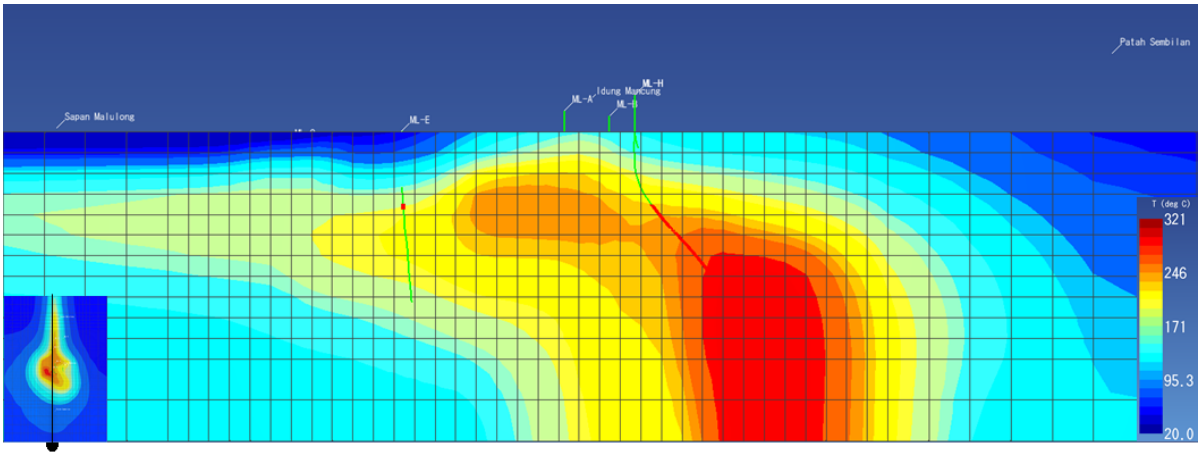

Figure 7: A north-south cross section of the model natural state temperature distribution

3.2 Production History Calibration

During the production history calibration or history matching, the rocks fracture permeability values were fine-tuned until the model can replicate the measured pressure changes. When the fracture permeability structures changed during the history matching runs, the natural state run was repeated to ensure that the initial pressure and temperature are still in good agreement with the measured data.

A plot of pressure changes over time can be generated from the collection of PT shut-in data. Pressure at feed point or major permeable zone is extracted from each survey and plotted on one chart against time. Figure 8 shows how the pressure values at feed point of ML-A1 have been extracted to generate a profile of pressure changes with time. It appears that the pressure history obtained from the static PT surveys correlates with the well production history, showing a pressure buildup after the production stopped.

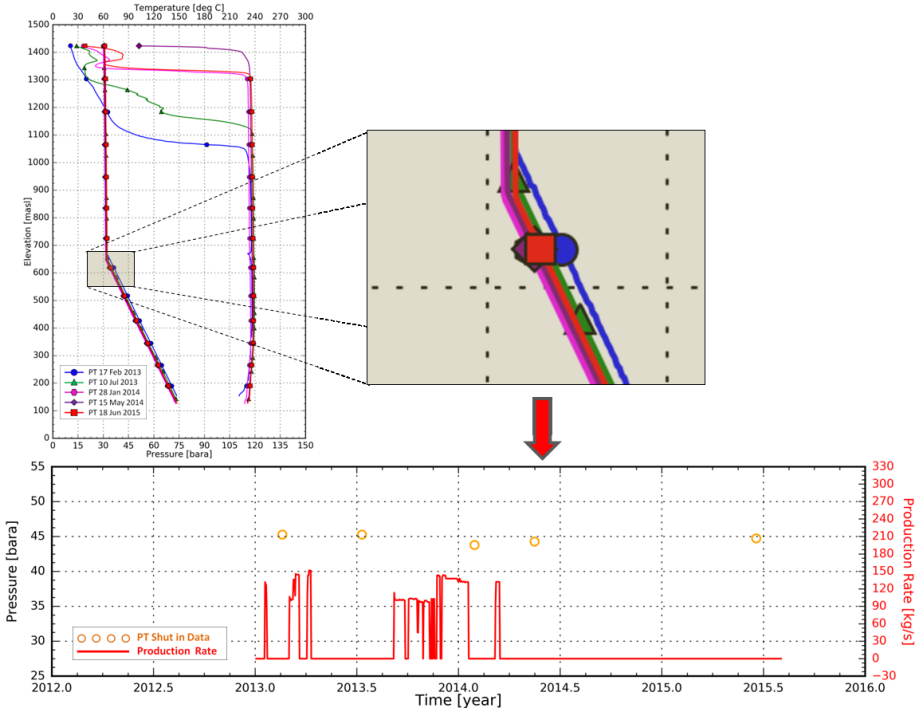

Figure 8: ML-A1 pressure changes record extracted from PT shut-in surveys collection

Furthermore, during the interference test, pressure changes were also recorded in the observation wells ML-B1 and ML-H1. The pressure data from capillary tubing obtained during the interference test was combined with the pressure changes recorded from the static PT surveys, which are presented in Figure 9.

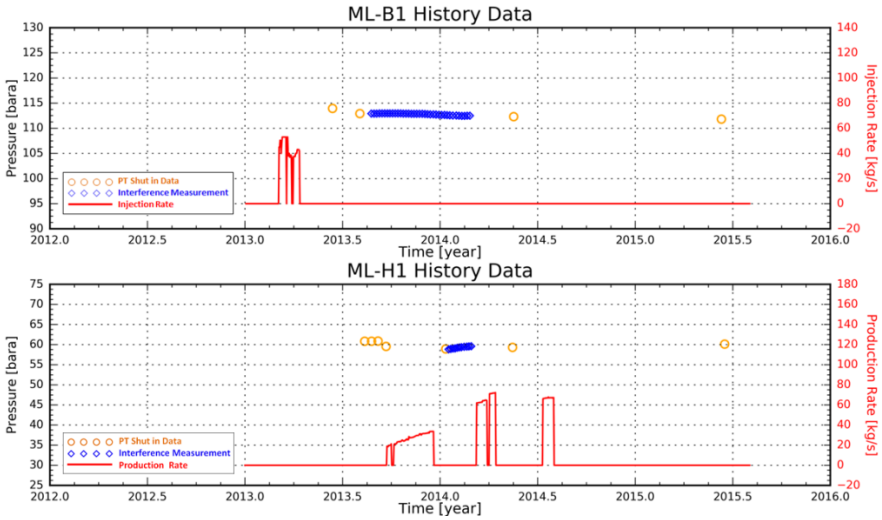

Figure 9: Pressure changes measured in the observation well

The calibration results are presented in Figure 10. A reasonable agreement between model and measured pressure changes was achieved by assigning fracture permeability distribution described earlier in Figure 5. Three permeability barriers (ROCK 7) were assigned, one is NEE-SWW direction and the other two are SE-NW, parallel one and another. The resulted fracture permeability and temperature structures infer that the southern deep heat sources mainly move upward through permeability of "high temperature" zone (ROCK4) and change direction through "high temperature and permeable" zone (ROCK3) before move laterally through "northern narrow permeable outflow" zone (ROCK2) and finally ascend to the surface. Due to the present of SW-NE permeability barrier, only a small fraction of the deep heat sources moving through ROCK5 & ROCK6.

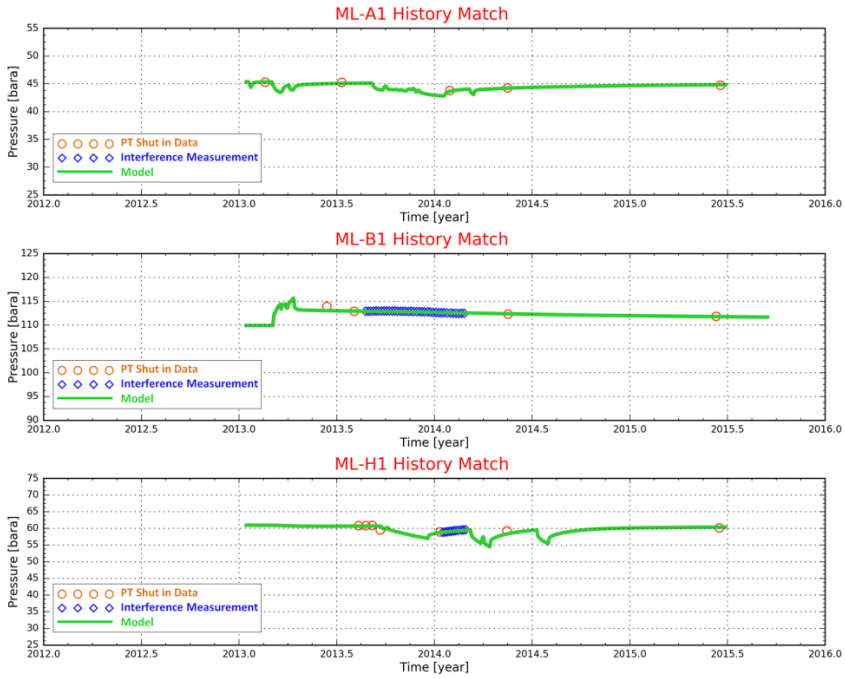

Figure 10: History matching results

4. FORECAST OF RESERVOIR PERFORMANCE

After the model calibrated by initial state and production history, it was then used to forecast reservoir response to exploitation under different development scenarios. Finally, the future reservoir performance forecasts were compared to select a preferred development scenario. An example is provided below to show how the model is used to perform such evaluation.

4.1 Development Layout

In this example, the ML-A and ML- H Pads are selected for production. The separator stations are put at Pad-A which is located downhill of Pad-H. The separated brine from the separator stations is transported to the pads ML-D, both located downhill from ML-A. Power plant condensate is injected into pad ML-B. Figure 11 below shows the assumed development layout.

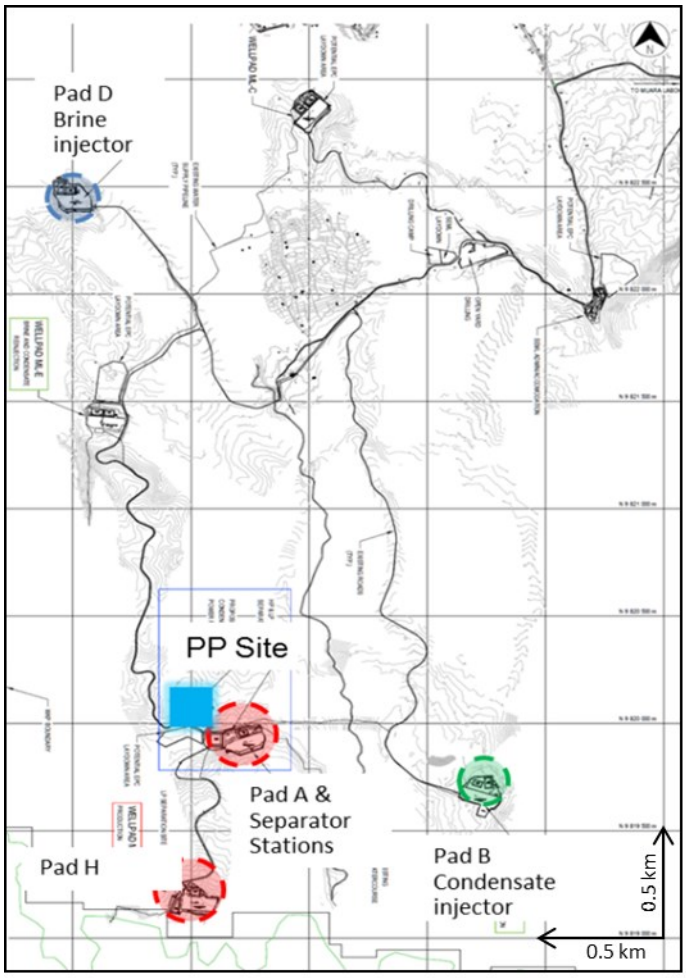

Figure 11: Field development layout

4.2 Assumptions

The field is assumed to utilize dual flash technology, allowing further production of steam at lower pressure (LP) from separated brine produced by high pressure (HP) production wells. At the same amount of energy extracted from two phase reservoir fluid, the dual-flash technology produces higher power generation compared to single flash plant. Steam demand, separation pressure, operating wellhead pressure (WHP), and operation availability assumptions of HP and LP systems are given in Table 1.

Table 1: Assumptions on HP and LP systems

Description	Unit	HP	LP
Operating WHP	Bara	10.1	5
Separation pressure	Bara	9.1	4.5
Turbine steam demand	kg/s	120	24.5
Availability	%	96	96

Steam deliverability of a geothermal well depends on reservoir fluid enthalpy, productivity index (PI, a measure of reservoir permeability), reservoir pressure, and casing geometry. In wellbore modeling, all those factors are processed to estimate well steam deliverability. Presently, production capacity of future production wells in Muara Laboh is still uncertain as reflected by the wide range

of production capacities of two wells completed inside the reservoir. The main uncertainties lies on the permeability (PI) and fluid enthalpy wells would encounter in the targeted reservoir. To define a reasonable assumption on average initial well steam deliverability of future wells, a Monte Carlo simulation, involves wellbore modeling, is carried out.

The future well is modeled to have encountered shallow and deep fractures (feedzones) at around 1000 and 1400mMD respectively. The shallow feedzone is assumed two-phase with enthalpy ranging from 1043 to1559 kJ/kg, while the deep feedzone is assumed liquid with 1038 to1110 kJ/kg enthalpy range. The productivity index (PI) values of shallow and deep feedzones are in the range of 1-90 kg/s-bar and 1-20 kg/s-bar respectively. Big hole casing configuration is used, with 13 3/8" production casing set at around 800mMD. A chance of well penetrating each feedzone is assigned 80%. This is translated into a modeling computation in that whenever a random number value is higher than 0.8, the corresponding feedzone will not be active (i.e. it will not be contributing to a well flow). If both feedzones are not active, the estimated production capacity will be equal to zero. Fluid enthalpy, productivity index (PI), reservoir pressure, feed-zone locations, and casing configuration used in the calculation are presented in Figure 12. These input values are decided base on the drilling and well testing data collected during the exploration program.

FZ1 (Two Phase)	**Min**	**Max**
Depth [masl]	650	
Depth [mMD]	1007	
Pressure Res [bar]	32.00	
Temp [deg C]	237	
Dryness [%]	1%	30%
Enthalpy [kJ/kg]	1043	1559
PI [kg/s.bar]	1	90
Success Ratio	80%	
FZ2(Liquid)	**Min**	**Max**
Depth [masl]	350	
Depth [mMD]	1431	
Pressure Res [bar]	56.40	
Temp [deg C]	235	255
Enthalpy [kJ/kg]	1014	1110
PI [kg/s.bar]	1	20
Success Ratio	80%	
Other Parameters		
WHP Target [bar]	10.1	
Separator Pressure [bar]	9.1	
#trials	10000	

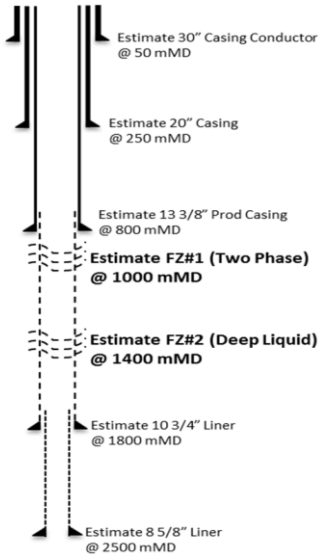

Figure 12: Assumptions used in wellbore model for future well initial steam deliverability calculation

Well is set to flow at operating wellhead pressure 10.1 bar and separation pressure 9.1 bar. A total of 10000 computation trials were done to generate the initial steam deliverability probabilistic curve shown in Figure 13.The modeling outcome shows initial steam deliverability of 15.6, 30.3, and 44.1 kg/s at the probability of occurrence P90, P50, and P10 respectively. For this instance, the P90 value of 15.6 kg/s is assigned as future well average initial steam deliverability assumption in the forecast simulation.

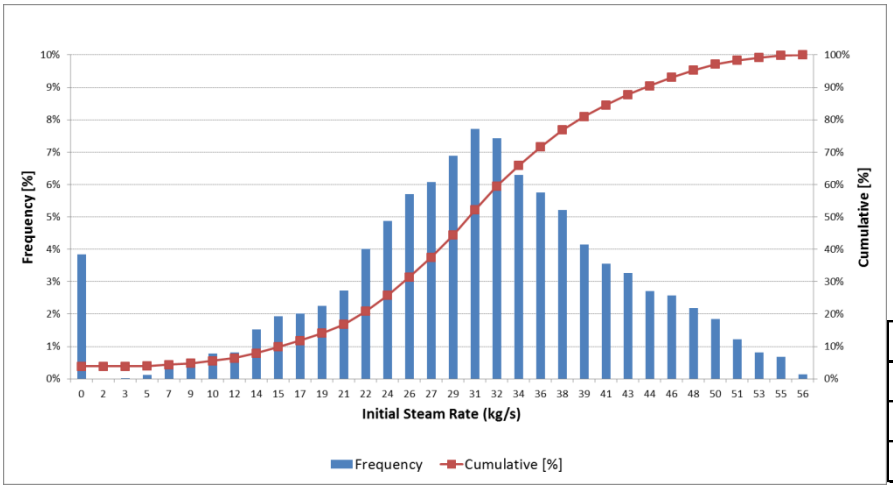

Probability	Initial Steam Rate (kg/s)
P 10	44.1
P 50	30.3
P 90	15.6

Figure 13: Probabilistic curve of future well initial steam deliverability estimates

Table 2 summarizes brine injection temperature, condensate injection flow rate, condensate injection temperature, and average initial well steam deliverability assumptions. Location of production and injection wells in the simulation grids is given in Figure 14. Production wells are put in the "high temperature" and "high temperature and permeable" zones. Brine injection wells are assigned in the "northern narrow permeable outflow", around 2 km from the closest production well.

Table 2: Production and injection well assumptions

Description	Unit	Value
Brine injection temperature	°C	144
Condensate injection flow rate	kg/s	35
Condensate injection temperature	°C	37
Average initial well steam deliverability	kg/s	15.6

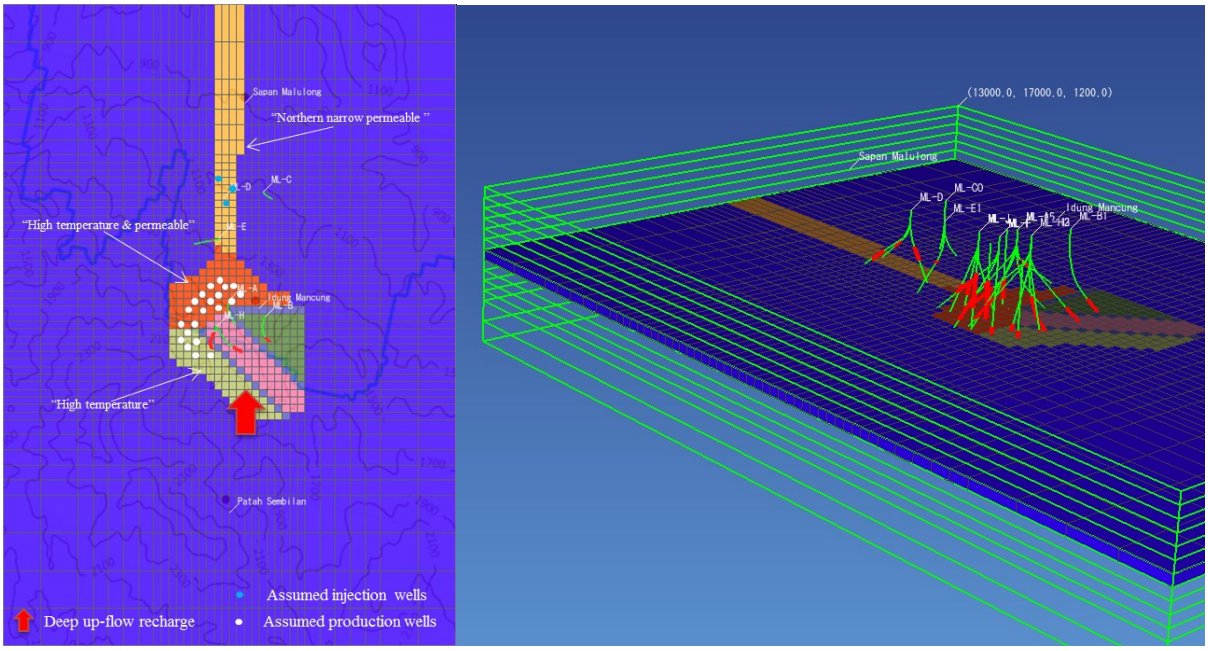

Figure 14: Location of future production and injection wells in the numerical model

4.3 Methodology

The methodology designed and applied allows more realistic forecast simulation.

1. All assigned production wells are constrained to operate at a constant 10.1bar WHP for HP and 5bar for LP throughout the life of the project. This is done by coupling the numerical model with a wellbore model.

2. At the beginning of simulation, each individual well Productivity Index (PI) value is adjusted to meet the assumed steam deliverability 15.6 kg/s. As the simulation is executed (i.e. reservoir exploitation begins), the steam deliverability of individual well is updated every three months following the pressure and enthalpy changes caused by the exploitation.

3. Total steam available of active wells of HP & LP systems are evaluated to obtain production decline. If total steam available is lower than steam demand, additional active well(s) (make up well) is put online.

4. Mass extraction imposed in the model is equal to 96% of the total HP & LP steam demand. If the total steam available is higher than the demand, the imposed production rate of all production wells is proportionally reduced.

5. If at some point in the future an HP well is no longer able to sustain production at required high pressure, the well can be switched to feed the LP system.

6. Brine injection flow rate is evaluated base on flowing enthalpy changes. Condensate injection flow rate is set constant.

Figure 15 presents the flowchart of simulation process. Forecast modules are created to allow communication between reservoir simulator and wellbore simulator as well as to run forecast simulation more automated.

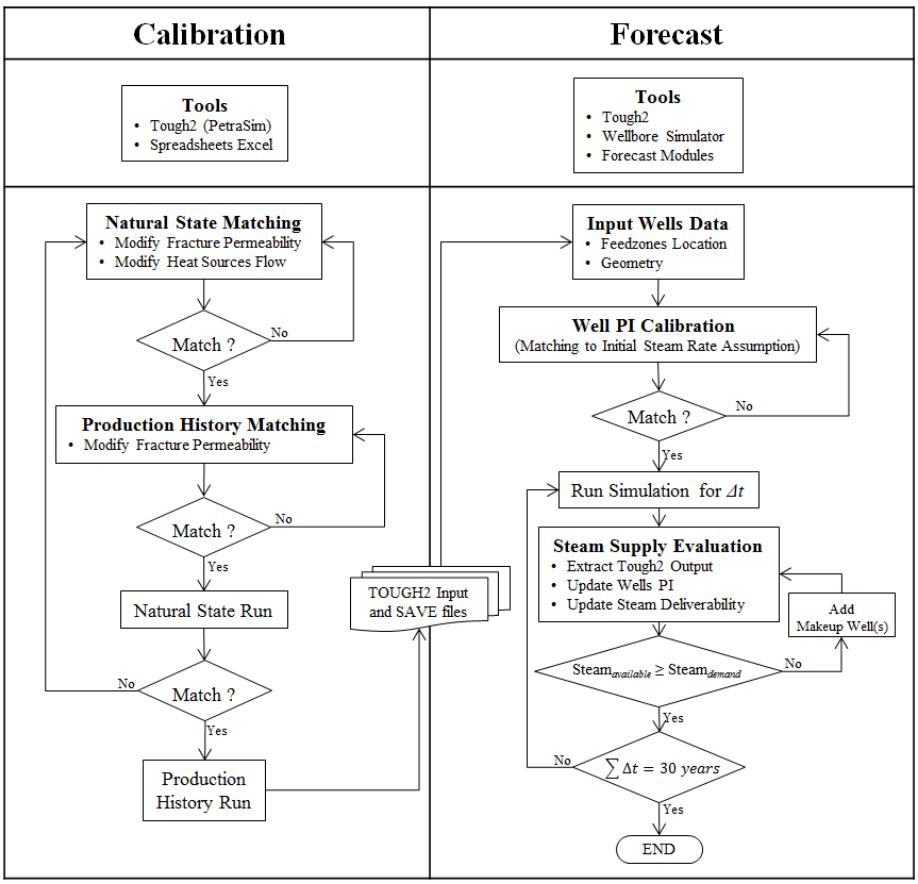

Figure 15: Simulation workflow

4.3 Production Scenarios

In this example, three cases are generated to evaluate the impact of different production wells extraction depth (shallow, deep, shallow & deep) to production performance. 'Shallow production' is defined for extraction above +500masl, while 'deep production' is defined if the main production zones are below +500masl. In all cases, brine is injected at Pad-D, and condensate is sent to ML-B1. In addition to two productive wells drilled during exploration program (ML-A1 and ML-H1), a total of additional eight (8) production wells are assumed to be drilled at the start-up. Table 3 shows the details of the scenarios.

Table 3: Generated development scenarios

Case	Well Initial Steam Deliverability (kg/s)	Num of Production Well		Num of Injection Well	
		Pad-A (Exclude ML-A1) "Extraction Strategy"	Pad-H (Exclude ML-H1) "Extraction Strategy"	Pad-D (Brine)	Pad-B (Condensate)
1	15.6	4 "Shallow&Deep"	4 "Shallow&Deep"	3	1
2	15.6	4 "Shallow"	4 "Shallow"	3	1
3	15.6	3 "Deep" 1 "Shallow&Deep"	4 "Shallow&Deep"	3	1

Shallow:	Extraction from above 500 masl
Deep :	Extraction from below 500 masl
Shallow&Deep:	Extraction from Shallow and Deep

4.4 Case 1: 30 Years Forecast Simulation

Figure 16, 17, and 18 below show the results of 30 years forecast simulation for the Case 1, including the steam supply schedule for HP and LP turbines for 30 years. The steam supply of HP & LP turbines can be fully sustained for 30 years by drilling a total of 21 production wells. Figure 16 shows the predicted production enthalpy is quite stable in the range of 1300 to 1350kJ/kg for 30 years production. The pressure decline and enthalpy changes have been translated into the steam field production decline and the corresponded make-up wells schedule as illustrated in Figure 18. Under this case, the first make-up wells drilling will be required after two (2) years production.

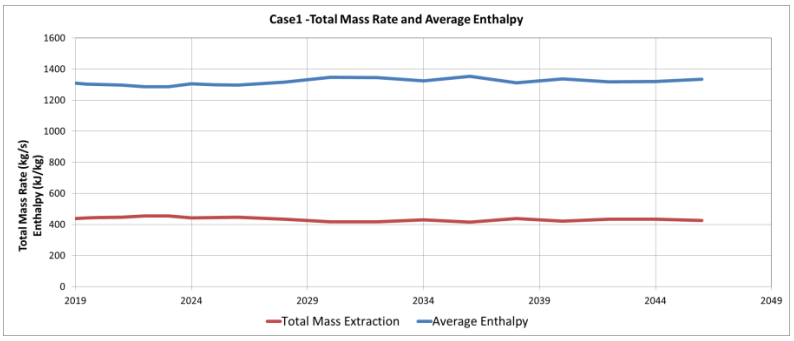

Figure 16: Case 1 total mass rate and enthalpy extracted for 30 years

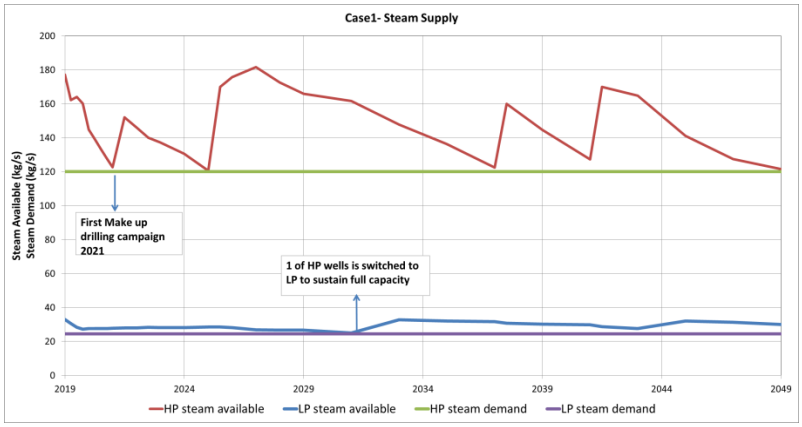

Figure 17: Case 1 steam supply forecast for 30 years simulation

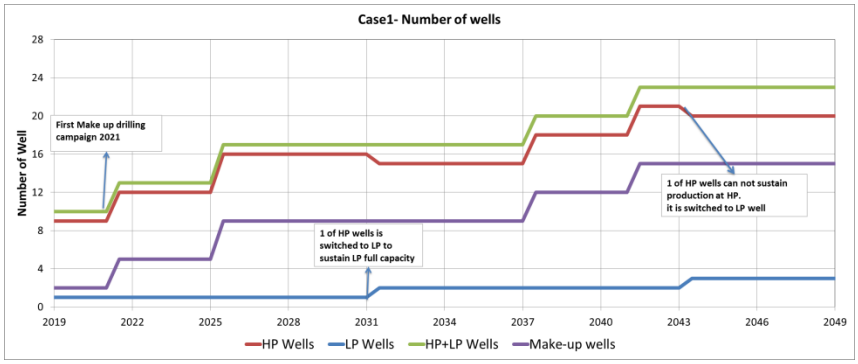

Figure 18: Case 1 production wells requirement to sustain 30 years steam supply

4.5 Strategies Comparison

Case 2 and Case 3 are run until the first time steam available reaches zero steam buffer, or in other word until the first make up well drilling is required. The longer the first make-up wells drilling campaign can be delayed, the better the production performance of the start-up wells. Figure 19 shows the results of forecast simulation of all cases presented in the form of field production decline with time. Case 2 has the highest production decline rate, needing make-up wells to be drilled in less than a year after start-up. This is the case where all production is from shallow and two-phase feed zones. Case 3, where fluid production is from both shallow two-phase and

deep liquid reservoir, gives the lowest production decline. In this case, make-up wells drilling can be delayed by up to five (5) years after start-up. It is interesting to note that whenever the portion of deep extraction increases, production decline decreases and therefore make-up wells drilling can be delayed longer.

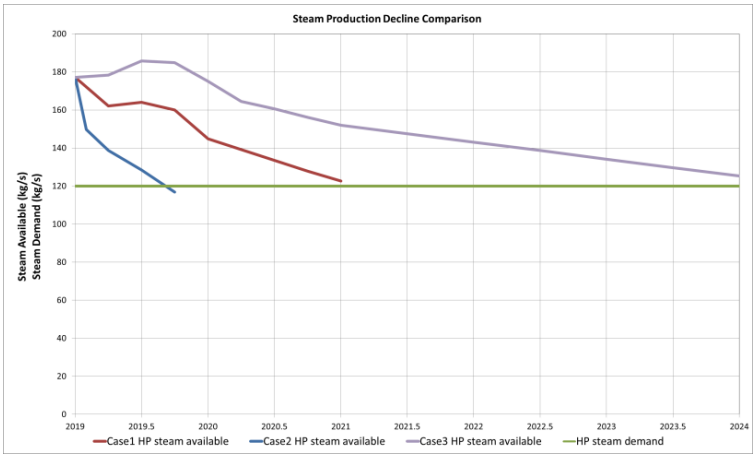

Figure 19: The results of forecast simulation in the form of filed wide production decline for all production cases

The analyses show that having more extraction from deep liquid reservoir will sustain steam supply longer before drilling make-up well is required. Therefore, for this particular example, it is recommended that future production wells be targeted both to shallow and deep reservoir (below 500masl).

5. CONCLUSION

From this reservoir simulation work the following conclusions can be drawn:

1. Reservoir simulation has been applied to assess fracture permeability distribution of Muara Laboh field using dual porosity formulation.
2. The numerical model has been successfully calibrated to initial state and production history data.
3. A workflow has been designed and applied to enable more realistic forecast simulation
4. The applied workflow has allowed different development scenarios to be assessed thoroughly, enabling a careful recommendation for field development plan to be made.

ACKNOWLEDGEMENTS

The authors wish to thank the management of SEML for the permission to publish this paper. Discussions with SEML Subsurface team members are very much appreciated.

REFERENCES

Itoi, R., Kumamoto, Y., Tanaka, T., and Takayama, J.: History Matching Simulation of the Ogiri Geothermal Field, Japan, *Proceedings*, World Geothermal Congress 2010, Bali, Indonesia (2010).

Supreme Energy Muara Laboh: Muara Laboh Geothermal Power Project-Stage 1 Development Feasibility Study, Unpublished Report, (2014).

Supreme Energy Muara Laboh: Muara Laboh Development Drilling Strategy, Unpublished Report, (2016).